# Ad-hoc modifications of cyclic mimetics of SOCS1 protein: Structural and functional insights

Sara La Manna [a], Sara Fortuna [b], Marilisa Leone [c], Flavia A. Mercurio [c], Ilaria Di Donato [a], Rosa Bellavita [a], Paolo Grieco [a], Francesco Merlino [a], Daniela Marasco [a,*]

[a] Department of Pharmacy, University of Naples "Federico II", 80131, Naples, Italy
[b] CONCEPT Lab, Istituto Italiano di Tecnologia (IIT), Via E. Melen, 83, I-16152, Genova, Italy
[c] Institute of Biostructures and Bioimaging, CNR, 80145, Naples, Italy

ARTICLE INFO

*Keywords:*
Mimetic peptides
Cytokine signaling
JAK/STAT
SOCS1
Cyclic peptides

ABSTRACT

Suppressors of cytokine signaling 1 (SOCS1) protein, a negative regulator of the Janus kinase (JAK)-signal transducer and activator of transcription (STAT) pathway, possesses a small kinase inhibitory region (KIR) involved in the inhibition of JAK kinases. Several studies showed that mimetics of KIR-SOCS1 can be potent therapeutics in several disorders (e.g., neurological, autoimmune or cardiovascular diseases). In this work, starting from a recently identified cyclic peptidomimetic of KIR-SOCS1, icPS5(Nal1), to optimize the peptide structure and improve its biological activity, we designed novel derivatives, containing crucial amino acids substitutions and/or modifications affecting the ring size. By combining microscale thermophoresis (MST), Circular Dichroism (CD), Nuclear Magnetic Resonance (NMR) and computational studies, we showed that the cycle size plays a key role in the interaction with JAK2 and the substitution of native residues with un-natural building blocks is a valid tool to maintain low-micromolar affinity toward JAK2, greatly increasing their serum stability. These findings contribute to increase the structural knowledge required for the recognition of SOCS1/JAK2 and to progress towards their conversion into more drug-like compounds.

## 1. Introduction

The Janus kinase (JAK)-signal transducer and activator of transcription (STAT) pathway is crucial in the transduction of cytokines intracellular signalling and is involved in the regulation of growth, haematopoiesis, development of immune, stem cells and mammary glands [1]. Delayed and/or incorrect functioning of JAK/STAT pathway may lead to the onset of pathological conditions, such as inflammatory and tumorigenic states [2]. Therefore, targeted therapies focused on restoring its physiological conditions have attracted extensive widespread attention in recent years [3]. Suppressors of Cytokine Signalling (SOCS) proteins can control JAK/STAT to promote the reduction of inflammatory hallmarks, including apoptotic genes and the maintenance of a dynamic equilibrium between cell proliferation and apoptosis for its own correct functioning [4]. The SOCS family consists of eight members. SOCS1 is an essential regulator of immune homeostasis and subverter of inflammation [5]; it can regulate responses of type I interferons (IFNs), which function through IFNAR1,2 and TYK2, JAK1 axes and type II IFNs (IFN γ), through IFNGR1,2 and JAK1,2 [6]. Additionally, SOCS1 modulates the signaling of interleukin (IL)-12, glycoprotein (gp) 130, IL-6, leukemia inhibitory factor (LIF) and common γ chain (CD132) through IL-2 and IL-21 [5]. SOCS1 is a major intracellular negative checkpoint of adoptive T cell response [7] and its deficiency or dysregulation is correlated with a number of immune disorders in humans, including systemic lupus erythematosus, scleritis and asthma [8,9]. Since immune responses contribute to autoimmunity/inflammation and cancer, the potential uses of SOCS1 mimetic peptides or of gene therapies are considered powerful therapeutic approaches [10]. For example, by comparing the antitumor effects of SOCS1 with type I JAK inhibitor (JAKin), the adenoviral-expression of SOCS1 demonstrated able to better decrease the proliferation of oral squamous cell carcinoma (OSCC) lines and induced cell cycle G2/M phase arrest and apoptosis [11].

SOCSs physically block the interaction of STATs with receptors through a proper interaction of their SH2 domains with phosphotyrosines of the cytoplasmic portion of the receptors. In addition, through a C-terminal domain (box), SOCSs can promote a proteasomal

* Corresponding author.
*E-mail address:* daniela.marasco@unina.it (D. Marasco).

Accepted 14 September 2022

degradation that determine the ubiquitination of the SH2 of substrates through the SOCS box-Elongin B/C complex [12]. Among different members, only SOCS1 and 3 can also inhibit JAKs' activity thanks to the direct interaction of a kinase inhibitory region (KIR) with Janus enzyme [13] and the interaction of JAKs with KIR-SOCS1 causes a reduction of p-JAKs and p-STATs levels [14]. From the crystal structure of the SOCS1/JAK1 complex [15], it was highlighted that KIR targets the substrate-binding groove of JAK with high specificity and thereby blocks phosphorylation, acting as "pseudosubstrate" of Tyrosine-kinase where $His^{54}$ mimics the tyrosine of the substrate [15]. Mutagenesis studies indicated that KIR of SOCS1 is a highly evolved inhibitor of JAK, and the mutation of any residue implied a significant decrease of binding affinity [15]. In detail, the fragment $His^{54}$-$Phe^{55}$-$Arg^{56}$-$Thr^{57}$-$Phe^{58}$-$Arg^{59}$ appeared crucial and its Ala-mutation lead to a higher $IC_{50}$ for JAK1. More specifically, $Arg^{56}$ and $Arg^{59}$ form hydrogen bonds with $Asp^{1040}$ of JAK1 that in molecular dynamics (MD) simulations studies, appeared to resist to external force disturbances. Although electrostatic interactions were the main driving force for the interaction, the non-polar residues $Phe^{58}$ and $Phe^{55}$ provided the greatest contribution to the binding [16].

In our previous studies, the truncation of KIR sequence (SOCS1 52–67 fragment), along with a "combinatorial focused library" screening approach, led to the discovery of a lead compound, named PS5, **1** (Fig. 1) [17–19].

With respect to KIR precursor, PS5 presented the $His^{54}$/Cys(Acm), $Phe^{55}$/Arg and $Arg^{56}$/Gln substitutions, and proved to act as good mimetic of SOCS1 biological functions in both cellular and *in vivo* environments [20–24]. Being PS5 a linear peptide, and thus intrinsically flexible, the construction of a pharmacophoric model resulted quite difficult, thus several cyclic analogues were designed and analyzed [24–27]. One cyclic analogue of PS5, bearing a lactam bridge between side chains of Asp (naturally occurring at position 52) and Lys (in replacement of $Ser^{60}$) residues, along with the replacement of $Phe^{58}$ with the non-natural L-1-naphthylalanine [Nal(1')], was developed and named icPS5(Nal1) (**2**). Such derivative showed the highest affinity toward JAK2 and the longest lasting biological effects in cells, where it reduced STAT1 migration and NADPH oxidases genes and increased *Sod1* and *Cat* antioxidant genes [28].

Therefore, based on the potential of lactam-bridged cyclic derivatives of PS5, in this work we designed and synthesized new icPS5 (Nal1) analogues, featuring key amino acids replacements and/or modifications affecting the ring size (including amide inversion). Our efforts were aimed to explore larger chemical diversities and to provide a new library of cyclic peptides that could implement the structure-activity relationships (SAR) information related to PS5 and PS5/JAK2 interaction. These compounds were thus analyzed conformationally by means of Circular Dichroism (CD), Nuclear Magnetic Resonance (NMR) and MD simulations, and functionally through microscale thermophoresis (MST) and serum stability assays.

## 2. Results and discussion

### 2.1. Design of internal cyclic PS5 analogues

Our previous studies focused on the development of cyclic decapeptidomimetics of PS5 pointed out that the insertion of a lactam bridge between the side chains of the $Glu^{1}$ and $Lys^{9}$ (peptide

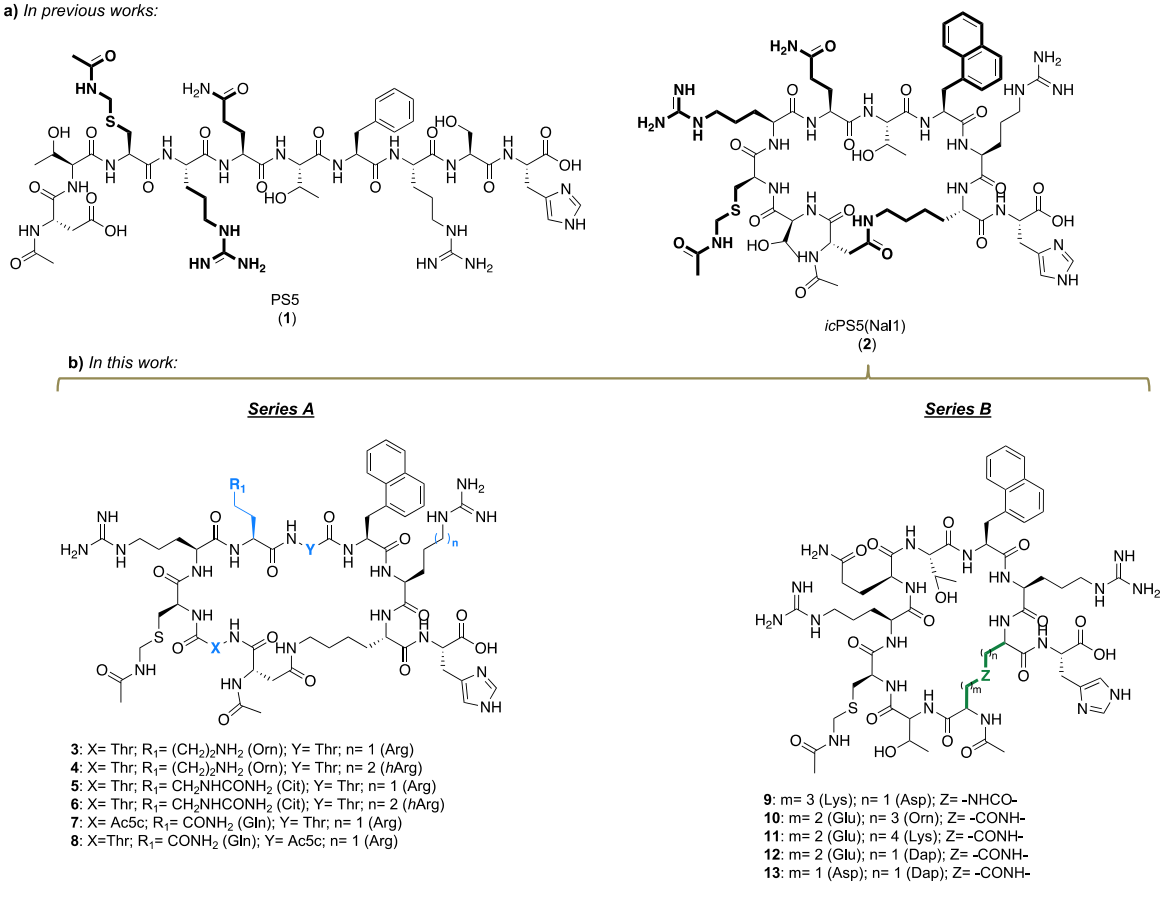


**Fig. 1.** Design of icPS5(Nal1) analogues. (a) Structures of previously described PS5 (**1**) and icPS5(Nal1) (**2**), where modified residues compared to $KIR^{52\text{-}61}$ of SOCS1 are depicted in bold; (b) in this study, icPS5(Nal1) was subjected to an optimization design, by exploring both key residue replacements (series A, peptides **3**–**8**) and ring bridge modifications (series B, peptides **9**–**13**).

numeration, Table 1) conferred enough conformational constraint to be investigated through NMR. Moreover, the simultaneous introduction of an additional unconventional amino acid (besides Cys(Acm) at position 3, deriving from the deconvolution of combinatorial libraries) such as Nal(1') in position 7 in place of the native Phe [28], led to the discovery of peptide **2**, icPS5(Nal1) (Fig. 1). In this study, we assumed compound **2** as reference and several point modifications were introduced within it by replacing few native residues with unconventional amino acids. Changes were driven by previous SARs [28] and chemical modifications aimed at the alteration of the cycle size, as global constraint [29] and the insertion of α,α-dialkylated residues, as local constraints [30,31]. Hence two series, A and B, of analogues were developed. In series A, residues replacements involved both Gln at position 5 (in compounds **3**–**6**) and three native residues: two Thr, at positions 2 and 6, and one Arg at position 8. To induce further conformational constraints threonines were replaced with Ac5c (2-aminocyclopentanecarboxylic acid) (compound **7** and **8**), while, to vary the distance between the positive guanidinium group of the side chain and the peptide backbone (compounds **4** and **6**), Arg was replaced with hArg (homo-arginine). In series B, the analogue compounds featured the inversion of residues involved in the lactam-bridge (compound **9**) or different cyclizing side chains, deriving from Glu, Orn and Dap substitutions (compounds **10**–**13**). A schematic structure of designed cycles is reported in Fig. 1 and their sequences in Table 1.

In major detail, in the series A, we mutated residues $Gln^5$, $Arg^4$, $Thr^2$ and $Thr^6$ that in protein numeration were at 56, 59, 53 and 57 positions, respectively. As single substitution, we mutated the amide group of $Gln^5$ side chain with the primary amine of Orn (ornithine) and the urea-like group of Cit (citrulline). In double mutated sequences, we investigated the substitution of $Arg^4$ with its longer analogue hArg. In the same library, we evaluated the effect of the introduction of Ac5c. This constrained residue is reported to reduce conformational flexibility of peptidomimetics and to enhance the structural specificity of recognizing compounds [32,33], it was placed in substitution of $Thr^2$ and $Thr^6$ that, in mutagenesis studies, did not appear crucial for the interaction with JAK2 [15].

In the series B, the size of the cycle was altered by substituting the side chains of $Glu^1$ and $Lys^9$. In these compounds, still maintaining a primary amine required for lactam formation, we reduced the alkyl chain of Lys ($(CH_2)_4$) by substituting it with of 2,3-diaminopropionic acid (Dap) [34] with one $CH_2$ and Orn with $(CH_2)_3$. Similarly, we restricted the alkyl moiety bearing the carboxylic acid by changing Glu, bearing $(CH_2)_2$, with Asp featuring only one $CH_2$. We also evaluated the effect of the reversion of the bridge deriving from an exchange of positions of Lys and Glu at the extremities. This peptide, even if reported in the B series, has the same cycle size of analogues of the A series and, in subsequent studies, will be compared to compounds of the first group.

### 2.2. *Binding affinity investigations*

Analogues of compound **2** were employed as ligands in *vitro* MST experiments, to evaluate their ability to recognize JAK2 catalytic domain [35]. Compounds of the series A demonstrated to bind to JAK2 with $K_D$ values quite similar to that previously reported for *ic*PS5(Nal1) ($K_D$ ~36 μM) [28]. Indeed, among them, both single and double mutations did not negatively affect the recognition providing dose-response curves of MST signals as reported in Fig. 2 A-B.

Signals reached saturation with fitted $K_D$ values in the same order of magnitude (Table 1). In particular, a slight improvement in terms of affinity can be highlighted in compound **6** where the two non-natural amino acids, Cit and hArg, presenting longer side chains with respect to native Gln and Arg, respectively, can allow an easier accommodation of the SOCS1 mimetics in the JAK2 binding site. Conversely, the local constraint introduced at positions 2 and 6 for the introduction of Ac5c (compounds **7** and **8**), decreased the ability to recognize JAK2 of a 10-fold value (without reaching a complete saturation, as reported in Fig. 2C): this is likely due to an excessively forced conformation that can partially mask hot spots of interaction. A similar $K_D$ was observed for compound **9** (Table 1) where, instead, the major random content (see below) limits the formation of specific interactions with JAK2. For the compounds of the series B, the different cycle lengths greatly affect the ability to interact with JAK2 causing $K_D$ values very high or indeed even

**Table 1**
Analogues of peptide **2**. Names, sequences, and $K_D$ values toward JAK2 catalytic domain, through MST assay.

| Series | Compound | Sequence | $K_D$ (μM) |
|---|---|---|---|
| A | **2** | Ac-D$^1$TC(Acm)RQTNalRK$^9$H-$NH_2$ | (3.6 ± 1.5)*10 |
| | **3** | Ac-DTC(Acm)ROrnTNalRKH-$NH_2$ | (3.2 ± 1.3)*10 |
| | **4** | Ac-DTC(Acm)ROrnTNalhArgKH-$NH_2$ | (3.9 ± 0.8)*10 |
| | **5** | Ac-DTC(Acm)RCitTNalRKH-$NH_2$ | (3.6 ± 0.9)*10 |
| | **6** | Ac-DTC(Acm)RCitTNalhArgKH-$NH_2$ | (3.1 ± 1.3)*10 |
| | **7** | Ac-DAc5cC(Acm)RQTNalRKH-$NH_2$ | (2.6± 2)*$10^2$ |
| | **8** | Ac-DTC(Acm)RQAc5cNalRKH-$NH_2$ | (1.2± 0.2)*$10^2$ |
| B | **9** | Ac-KTC(Acm)RQTNalRDH-$NH_2$ | (1.6 ± 0.3)*$10^2$ |
| | **10** | Ac-ETC(Acm)RQTNalROrnH-$NH_2$ | No binding |
| | **11** | Ac-ETC(Acm)RQTNalRKH-$NH_2$ | (5.2 ± 0.5)*10 |
| | **12** | Ac-ETC(Acm)RQTNalRDapH-$NH_2$ | (7.1 ± 2)*10 |
| | **13** | Ac-DTC(Acm)RQTNalRDapH-$NH_2$ | No binding |

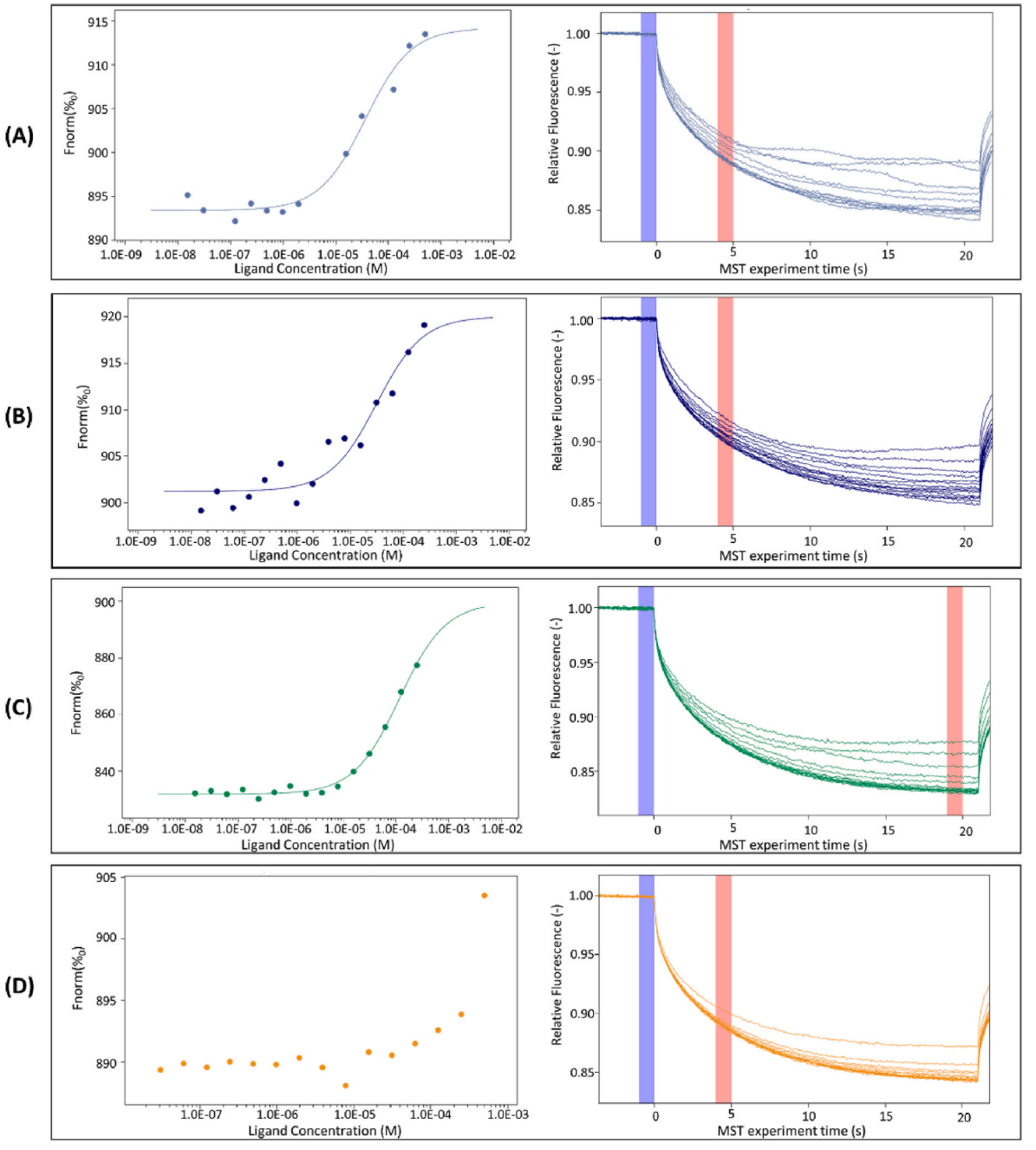


**Fig. 2.** In vitro binding assays. Binding isotherms for MST signals versus peptides concentrations (left column) and thermophoretic traces of MST assays for the binding to JAK2 (right column) of peptide (A) **5**; (B) **6**; (C) **8**; (D) **13**.

not quantifiable. In detail, compounds presenting a reduced C-terminal arm of the bridge (**13** (Fig. 2 D) and **10**) did not provide suitable MST variation for fitting, in the same experimental conditions of other compounds.

### 2.3. Conformational studies

#### 2.3.1. Circular Dichroism

To evaluate the conformational properties of analogues of icPS5 (Nal1), CD studies were carried out and spectra are reported in Fig. 3.

Compound **2**, did not exhibit a canonical CD profile, as reported [28] (Fig. 3A), but a band centered at 230 nm is its peculiar feature and indicates an aromatic involvement in the cyclic structure likely due to the presence of the naphthyl moiety of Nal1, that is absent in the spectrum of its linear counterpart [24]. By analyzing spectra of the analogues of the series B (Fig. 3A), the two analogues containing hArg residue, **4** and **6**, do not present the aromatic band and this can be due to the longer side chain of hArg that enhances the flexibility of the backbone and limits the formation of π-π interactions. Conversely these interactions, appeared enhanced in analogues bearing Ac5c residue, in particular at position 6 (peptide **8**); this constrained β-residue is reported to limit conformational freedom and, in combination with α-amino acids, can promote the formation of helical structures in a way strictly dependent on adjacent residues [36]. This tendency is confirmed in our analogues **7** and **8**, whose spectra present a minimum at ~222 nm (Fig. 3B). The deconvolution of CD spectra reported in Table 2, supports for peptide **7** a good helical content, if compared with most part of other analogues. None of the listed features are present in the spectra of the cycle with inverted extremities, peptide **9**, where the absolute minimum at $\lambda < 200$ nm is indicative of a prevalent random content (Fig. 3B).

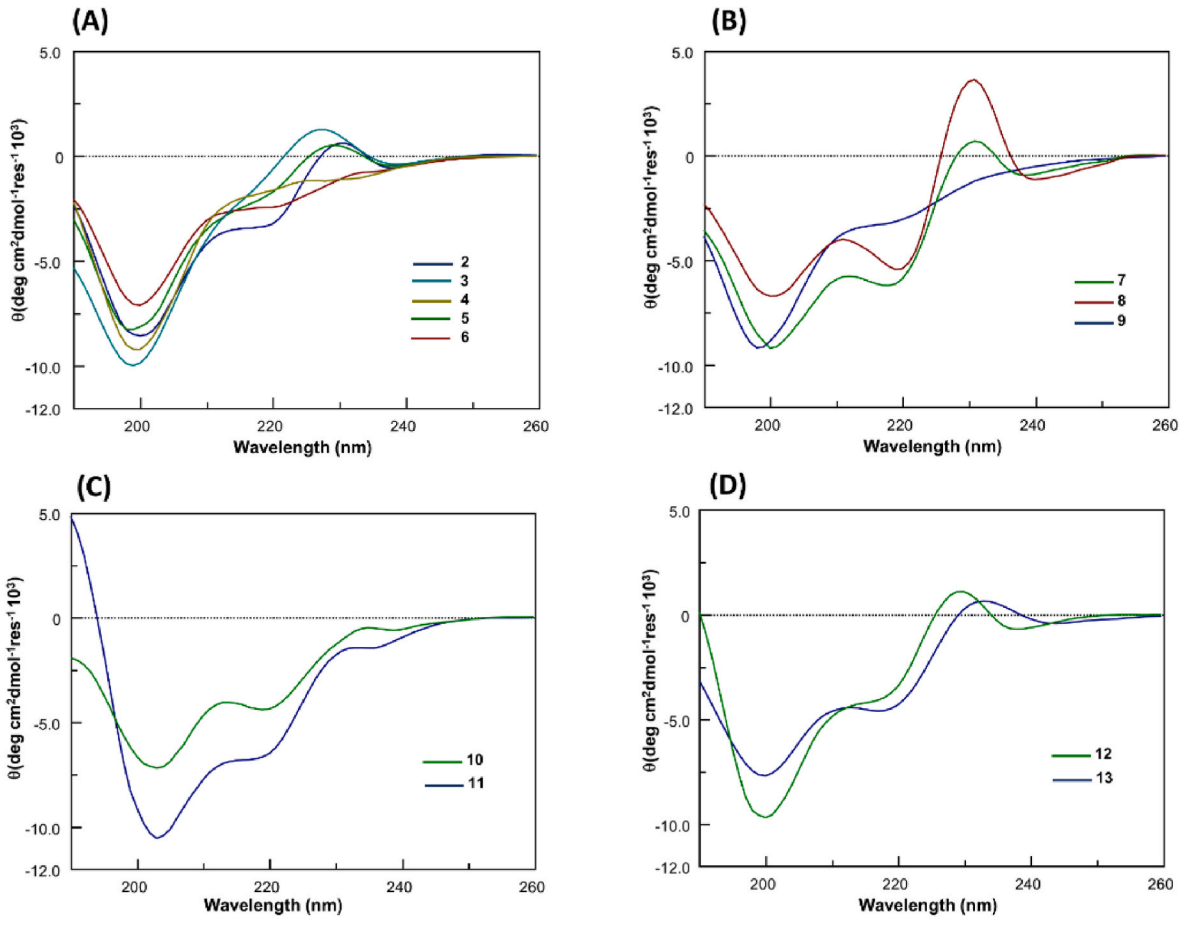


**Fig. 3.** Overlay of CD spectra of (A) **2**–**6**; (B) **7**–**9**; (C) **10**, **11**; (D) **12**, **13** peptides.

**Table 2**
Deconvolution of CD spectra of icPS5(Nal1) analogues.

| Peptide | Helix | Beta | Turn | Random Coil |
|---|---|---|---|---|
| 2 | 0.0 | 36.9 | 13.0 | 50.1 |
| 3 | 0.0 | 37.8 | 12.7 | 49.5 |
| 4 | 1.3 | 35.5 | 15.8 | 47.4 |
| 5 | 0.0 | 39.8 | 13.0 | 47.2 |
| 6 | 0.4 | 37.6 | 15.0 | 47.0 |
| 7 | 4.1 | 36.2 | 11.0 | 48.7 |
| 8 | 0.0 | 42.9 | 9.6 | 47.5 |
| 9 | 1.3 | 36.1 | 14.5 | 48.1 |
| 10 | 3.5 | 30.1 | 14.5 | 51.9 |
| 11 | 6.6 | 31.9 | 12.5 | 49.0 |
| 12 | 0.0 | 42.4 | 11.7 | 45.9 |
| 13 | 0.7 | 39.4 | 11.9 | 48.0 |

Concerning the other members of the series B, the overlay of spectra of **10** and **11** (Figs. 3C) and **12** and **13** (Fig. 3D), are reported, separately. Compounds **10** and **11,** that have a longer N-terminal arm, with respect to **2**, lack the aromatic band. This feature suggests a different orientation of aromatic residues as also indicated, especially for peptide **11**, by a certain helical content of these compounds (Fig. 3C and Table 2). Conformingly, TFE (2,2,2 trifluoroethanol) titration for peptide **11** (reported in Fig. S1) indicated that $\theta_{222nm}$ reached a saturated maximum helical content already at 30% TFE (v/v). Conversely, the reduction of the C-terminal portion of the bridge, for Dap/Lys substitution, allows the rescue of the aromatic band suggesting more rigid conformations in peptide **13**, that persists despite the elongation of N-terminal arm in the peptide **12** (Fig. 3D).

*2.3.2. NMR*

On the basis of combined results of MST and CD studies, several cyclic compounds of both groups were investigated through 2D [$^1$H, $^1$H] NMR spectroscopy, in conditions similar to those employed for compound **2**, i.e., in $H_2O/D_2O$ 90/10 (v/v) [28]. For **3**, **4**, **10** and **11** analogues proton resonance assignments were obtained by comparison of TOCSY [37] and ROESY [38] spectra (Figs. S2–S5, Tables S1–S4) and a few assignments (reported in red in Tables S1–S4) resulted ambiguous due to spectral overlaps and the flexibility of the studied systems. Specifically, the spectrum of peptide **4** resulted particularly affected by a conformational variability for the presence of duplicated spin systems (Fig. S3). As expected, the analysis of NOESY [39] and ROESY spectra indicated that all icPS5 analogues lack well-defined secondary structure elements, as also evidenced by inspection of ROEs patterns (Fig. S6): these contain mostly sequential contacts like $H_{Ni}$–$H_N$i+1, Hαi-$H_N$i+1 and a few Hβi-$H_N$i+1 contacts [40]. Structure calculations were performed with the software CYANA [41] and pointed out flexible cyclic conformations. For peptide **3**, NMR structures were obtained with 73 distance (46 intraresidue, 23 short- and 4 long-range) and 23 angular constraints, for compound **10** with 63 distance (38 intraresidue, 22 short- and 3 long-range) and 30 angular constraints, for analogue **11** with 80 distance (50 intraresidue, 26 short- and 4 long-range) and 30 angular constraints. Concerning peptide **4**, a tentative final structure calculation was obtained employing a reduced number of restraints (42 distance (25 intraresidue, 14 short- and 3 long-range) and 18 angular constraints) after the exclusion of ambiguous signals related to residue 5. Then, an unrestrained energy minimization protocol was implemented for the best 20 conformers composing the NMR conformational ensemble of each peptide to obtain structures reported in Fig. 4.

Upon this, peptide **3** showed an enhancement in secondary structure

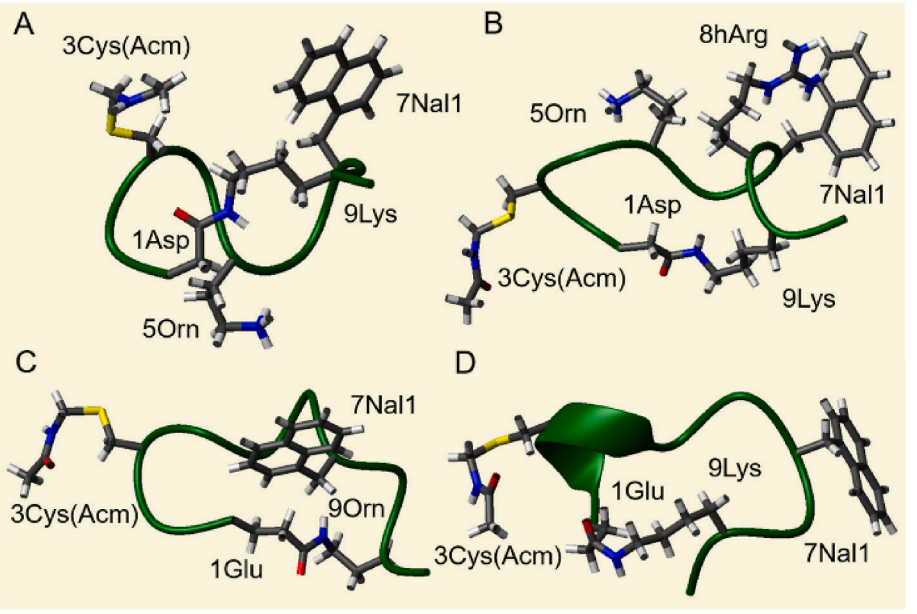


**Fig. 4.** NMR structures. First conformers (i.e., the ones better obeying to experimental restraints) of diverse NMR ensembles of structures for: (A) **3**, (B) **4**, (C) **10**, and (D) **11** analogues. The structures correspond to those calculated with CYANA subjected to unrestrained energy minimization. The side chains of residues involved in the lactam bridge and non-standard amino acids are shown.

elements, since 6/20 models presented a short $3_{10}$-helix in the region encompassing Asp[1]-Arg[4] and/or Thr[6]-Arg[8] (Fig. S7). In addition, compound **11** presented short $3_{10}$ helices but only in 2/20 structures (Fig. S8). Instead, **4** and **10** compounds still lacked distinct structuration elements (Figs. S9–10) despite minimization. Structures underwent a clusterization procedure with the software Chimera [42,43] by superimposing the twenty NMR conformers of each cyclic peptide on all atoms, with the exception of N- and C- terminal ends. Clusterization results suggested less conformational variability for peptide **3** with respect to other peptides: the 20 minimized conformers were clustered in 4 sub-families and the most populated one contained 15 models (Table S5). Peptides **4**, **10** and **11**, instead, were represented by 5, 6 and 5 subfamilies of conformationally related structures, respectively, and none of them is populated by a number of conformers higher than 7, further reflecting the flexibility of these cyclic peptides in aqueous environment (Tables S6–S8).

### 2.3.3. *Molecular modelling*

In addition to conformational analysis reported in previous sections, we performed several molecular modelling studies on cycles that presented the most interesting binding abilities: compounds **3** and **4** as bearing single and double mutations with $K_D$ values close to the icPS5 (Nal1) and compound **13** for its inability to bind JAK2. In more detail, these compounds were assayed for their capacity to inhibit SOCS1/JAK2 interaction, by targeting the same site of recognition on JAK2 targeted by KIR-SOCS1 (Fig. S11). From previous studies, it is known that JAK1 binds KIR primarily in the region from Val[1037] to Ser[1056] [15]. By aligning JAK1 to JAK2 (Fig. S12), this region corresponds to Val[1010]-Ser[1029] in JAK2. In this region, JAK1 residues known to be in direct contact to KIR are 11. Importantly, in the corresponding JAK2 region only 6 are conserved (Val[1010], Ser[1016], Pro[1017], Phe[1019], Leu[1026], Ser[1029]). To obtain initial icPS5(Nal1) analogues/JAK2 models, 1000ns long MD simulations were performed in water at 300K to allow each compound to explore its accessible conformations (Figure S13 A-C). The conformations were clustered to identify the most frequent backbone organization assumed by each peptide (insets in Figure S13 A-C). The identified conformers were docked to the KIR binding site on JAK2 (Figure S13 D-F). The docking procedures provided similar binding free energies, namely −5.0 kcal/mol for **4**, -4.7 kcal/mol for **3**, and -4.8 kcal/mol for **13**. To assess whether the icPS5(Nal1) analogues/JAK2 complexes were kinetically stable over time, MD simulations in water at neutral pH were carried out confirming the experimental $K_D$s reported in Table 1. Indeed, both **3** and **4** peptides did not leave the KIR binding site on JAK2 even after 500ns (Fig. 5A–B).

In more detail, during the simulated time compound **3** maintained a contact area of (4.2 ± 0.5) nm$^2$ with JAK2, while **4** showed a larger value of (5.5 ± 0.5) nm$^2$ (insets in Fig. 5A–B). Conversely, the compound **13** moved along JAK2 surface and partially left KIR-SOCS1 binding site on JAK2 (Fig. 5C) presenting an average contact area with JAK2 of (4.8 ± 0.8) nm$^2$. This large contact area, however, only partially overlapped with the KIR binding site. In addition, the fluctuations of the large contact area between **13** and JAK2 indicated a certain instability of the complex **13**/JAK2 (inset in Fig. 5C).

In its final conformation, cycle **4** appeared more tightly "sandwiched" to the JAK2 residues normally involved in KIR recognition with respect to compound **3**. This effect is observable in Fig. 5A–B where all icPS5(Nal1) analogues/JAK2 complexes are reported. Indeed, by looking at the minimum distances between PS5 analogues and the residues of JAK2 involved in KIR-SOCS1 recognition (Fig. 5D), cyclic compounds maintained their distances within 0.80 nm in the case of compound **4**, and within 0.50 nm from as many as five residues of JAK2 (namely Pro[1017], Ile[1018], Phe[1019], Leu[1026], Ser[1029]) during the simulation time. For **3** minimum distances appeared longer with respect to **4**, but always below 1.10 nm and in close contact (below 0.35 nm) to Thr[1027] and Glu[1028] JAK2 residues. As expected, peptide **13**, is not specific for KIR binding residues on JAK2, even if it is in close contact with Ile[1018], Phe[1019], Leu[1026], Thr[1027] its distance from Glu[1015], Ser[1016], Ser[1029] reached values larger than 1.0 nm indicating its separation from the binding site.

## 2.4. *Serum stability*

Serum stability assays were performed to evaluate the proteolytic stability of new icPS5(Nal1) analogues. In Fig. 6A–B, we reported the degradation profiles of compounds belonging to the series A and B, respectively. For 17 h, single mutated analogues, **2** and **3,** displayed a similar level of ~30% degradation while compound **5** of ~50%. After 42 h, peptide **3** appeared completely degraded. Doubly mutated

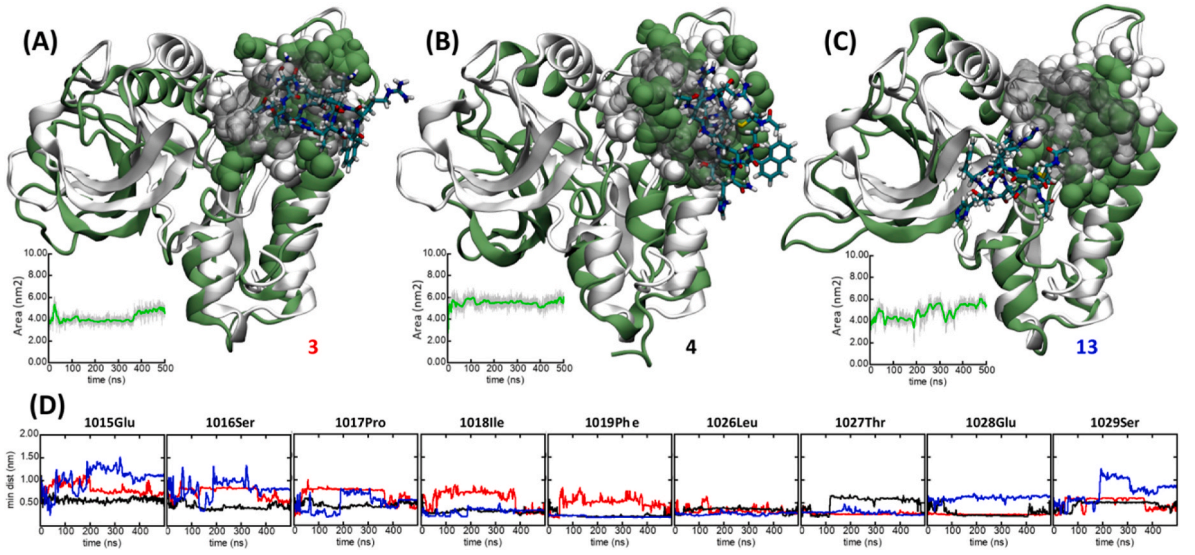


**Fig. 5.** MD Analysis. Comparison between the initial peptide position (whose surface area is represented by a grey shadow) as obtained by docking, and the same peptide after 500ns of molecular dynamics simulation (licorice) for (A) **3**, (B) **4**, and (C) **13**. JAK2 residues known to bind KIR are highlighted with their van der Waals spheres both on the initial (white) and final (green) JAK2 conformations. Water molecules and ions have been removed for ease of visualization. In the insets: time evolution of cyclic peptide contact area on JAK2, calculated as the half difference between the solvent accessible surface area (SASA) of the complex and that of the isolated peptide and JAK2, namely Area = [SASA(peptide)+SASA(JAK2)-SASA(complex)]/2. (D) peptide-JAK2 residues distance for peptides **3** (red), **4** (black), and **13** (blue).

compounds, bearing hArg (**4** and **6**) are more stable over time than the others. As expected, the insertion of the Ac5c residue (**7** and **8**) conferred an enhancement of stability to proteolytic degradation, almost comparable to analogues bearing hArg.

Interestingly, the inversion of Asp and Lys position in the bridge (peptide **9**) rendered the peptide extremely sensitive to proteases since they appeared completely degraded after 17 h. This effect was probably due to a major exposure of the lysine (last residue at the N-term) that favors endopeptidases that often hydrolyze the peptide bond by recognizing Arg and Lys residues. For the other analogues of series B (Fig. 6 B) it is evident that cycles **10** and **13** are more prone to degradation than **11** and **12** compounds that instead show a stability close to icPS5(Nal1), likely for the similarity of ring sizes. While for peptide **10**, the presence of a larger cycle induces increased flexibility and consequent exposure of residues subject to proteolytic degradation.

Digestion mixtures were also analyzed by LC-MS after 24 h: as common feature, as expected, MS analysis confirmed the stay of cyclic structures as prevalent species, along with the presence of compounds lacking His at position 10, that is not involved in the cycle (data not shown).

## 3. Conclusions

SOCS1 protein has an important potential therapeutic role in the treatment of autoimmunity and cancer [5]. Indeed, recently, the induction of SOCS1 expression allowed to increase the therapeutic efficacy of radiation in tumors presenting low SOCS1 levels [44]. Similarly, when overexpressed in COPD (chronic obstructive pulmonary disease), SOCS1 reduced the secretion of pro- and increased anti-inflammatory factors [45]. In addition, peptidomimetics of SOCS1-KIR exhibited great potentialities for immune-modulatory therapeutics [46,47]. Recently, the peritoneal administration of a peptide covering SOCS1-KIR, caused the inhibition of the progression of experimental autoimmune encephalomyelitis (EAE, a rodent model of multiple sclerosis) and mitigated experimentally induced uveitis in mice and rats through simple topical application in an eye drop form [48]. The employment of peptidomimetics revealed efficient as recently demonstrated by several pTyr-peptides derived from the JAK1 activation loop targeting the SH2 domain of SOCS1 [49].

In the context of KIR-SOCS1 analogues, we have developed and patented a cyclic peptidomimetic, icPS5(Nal1), bearing a lactam bridge between the side-chains of residues located at the extremities of the peptide backbone. Herein, following a medicinal-chemistry approach, we deeply investigated the structural and functional factors required for the recognition of JAK2 by a series of cycles with point mutations and different bridge sizes. For investigated compounds conservative substitutions seemed not to affect the recognition of JAK2 since they displayed binding affinities similar to that already registered for the compound **2**. Conversely, the introduction of a cyclopentane-based β-amino acid in two different positions reduced the affinity of the cycle of a 10-fold factor as well as the inverted cycle did. Structurally, the introduction of a cyclic β-residue caused a slight shift toward helical conformations while the inversion of the cycle induced a mainly random situation. These opposite conformational variations, however, implied minor binding capacity. This latter was completely lost in analogues with reduced ring size, *i. e.* **10** and **13** compounds, that, from NMR analysis, resulted endowed with great flexibilities and thus, unable to overlap to KIR SOCS1 recognition site on JAK2, as shown by MD simulations. This flexibility is also reflected in the major ease of degradation observed in the inverted cycle, **9**. The structural consequences of introduced modifications relied on the limitation but not the suppression of conformational flexibility of compounds as evident in the NMR and CD analyses, in them, the exposure level of aromatic naphthylalanine residue strictly depends on the applied chemical variation.

Actually small inhibitors of JAK proteins are clinically employed in proliferative neoplasia and in autoimmune diseases but the lack of selectivity among JAKs is a serious limitation for their application [10]. Thus, an alternative and prominent strategy is represented by the design and functional investigations of SOCS1 mimetics as novel therapeutic agents in diseases presenting hyperactivated JAK-STAT. Herein, presented results are crucial for the direct translation of the KIR-SOCS1 peptidomimetics, into specific inhibitors of JAK2, through the introduction of *ad hoc* chemical modification into well-established lactam cycles.

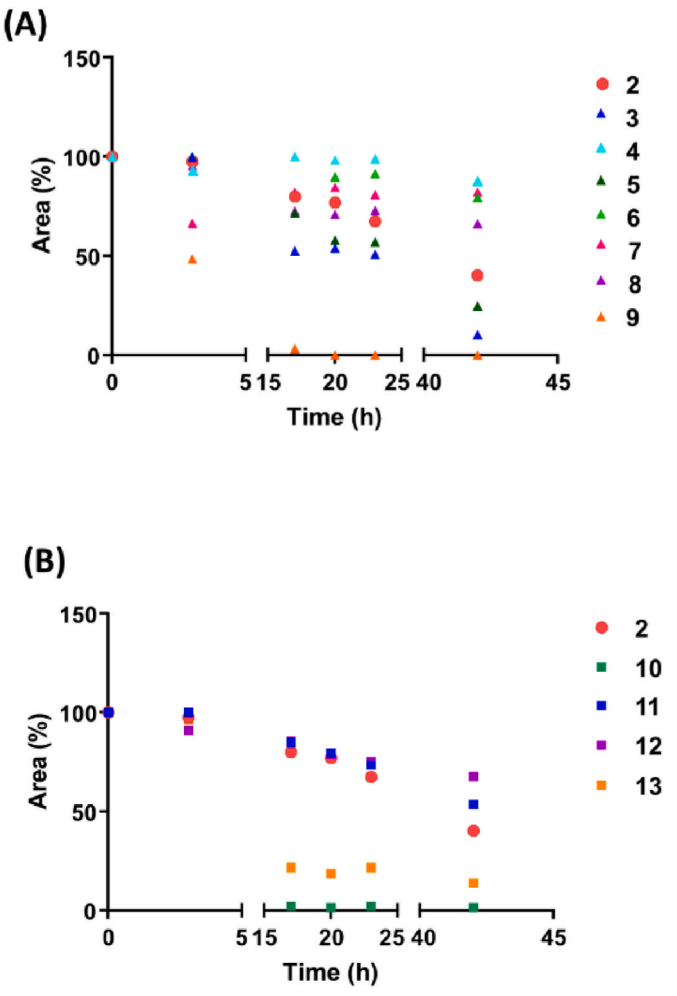


**Fig. 6.** Proteases' degradation profiles. Serum stability assay of peptide **2** analogues: (A) and (B) series, as reported in Table 1. The area of chromatographic peak at t = 0 min was assumed as 100% and residual areas at other time points were calculated as the percentage with respect to the area at t = 0 min.

## 4. Experimental

### 4.1. Peptide synthesis

Peptides were assembled stepwise on a 0.1 mmol scale Fmoc Rink amide resin (0.72 mmol/g as loading, 100–200 mesh as particle size) as already reported [24,50]. Peptides were than purified by preparative RP (Reverse-Phase)-HPLC, applying a linear gradient of 0.1% TFA $CH_3CN$ in 0.1% TFA water from 5 to 70% over 13 min with a semipreparative 2.2 × 5 cm C18 column at a flow rate of 20 mL/min, using a UV detector set at a wavelength of 210 nm. Peptides' purity and identity were confirmed by LC-MS and then they were lyophilized and stored at −20 °C until use. All compounds are >95% pure by HPLC (Figs. S14–S19).

Reagents for peptide synthesis were from Iris Biotech (Germany), solvents for peptide synthesis and HPLC analyses were from Romil (Dublin, Ireland); reversed phase columns for peptide analysis and the LC-MS system were from ThermoFisher (Waltham, MA).

### 4.2. Microscale thermophoresis experiments

MST experiments were performed with a Monolith NT 115 system (Nano Temper Technologies) equipped with 60% LED and 40% IR-laser power. Labeling of His-tagged Catalytic Domain of JAK2 (residues 826–1132) (Carna Biosciences) was achieved with the His-Tag labeling Kit RED-tris-NTA. Internal Cycle peptides were used starting from a stock solution of 1 mM in 50 mM Tris-HCl buffer (150 mM NaCl, 0.05% Brij35, 1 mM DTT, 10% glycerol) at pH 7.5 as already reported [51]. The dye concentration was adjusted to 100 nM while the protein concentration was 200 nM. Subsequently, protein and dye solutions were mixed and incubated in the dark for 30 min. To monitor binding of cyclic analogues, a serial dilution (1:1) was carried out by preparing 16 samples on average. Standard capillaries were employed for analysis.

The equation implemented by the software MO-S002 MO Affinity Analysis [52], used for fitting data at different concentrations, is based on Langmuir binding isotherm.

### 4.3. Circular Dichroism (CD) spectroscopy

Samples (200 μM) were prepared by dilution of freshly prepared stock solutions (1 mM peptide). CD spectra were recorded on a J-810 spectropolarimeter (JASCO, Tokyo, Japan), registered at 25 °C in the far-UV region from 190 to 260 nm. To each spectrum (obtained with an average of 2 scans), related blanks were subtracted, and the intensity was reported as average molar ellipticity per residue (deg*$cm^2$*$dmol^{-1}$*$res^{-1}$ as units). Spectra were acquired in 10 mM phosphate buffer at pH 7.4, in a quartz cuvette with a path-length of 0.1 cm [22]. For icPS5(Nal1) E/K (**11**), CD spectra were acquired in 10 mM phosphate buffer in mixtures with TFE (TFE/$H_2O$ 0–70% v/v) [22]. Deconvolutions of CD spectra were obtained by BESTSEL software (http://bestsel.elte.hu/) [53].

### 4.4. NMR spectroscopy

Conformational studies were performed by registering NMR 1D [$^1$H], 2D [$^1$H, $^1$H] TOCSY (Total Correlation Spectroscopy) [37], NOESY (Nuclear Overhauser Enhancement Spectroscopy) [39], ROESY (Rotating frame Overhauser Enhancement Spectroscopy) [38] and DQFCOSY (Double Quantum-Filtered Correlated Spectroscopy) [54] spectra on a Varian Unity Inova 600 MHz spectrometer provided with a cold probe. Spectra were acquired with 16–64 scans, 128–256 FIDs in t1, 1024 or 2048 data points in t2, and with the following mixing times: 70 ms for TOCSY experiments, 200 and 300 ms for NOESY experiments, 250 ms for ROESY experiments. Water suppression was obtained by *Excitation Sculpting* [55]. Peptide samples were prepared with a total volume of 540 μL $H_2O/D_2O$ 90/10 v/v and a final concentration of 1 mM, 1,3 mM, 938 μM, and 827 μM for **3**, **4**, **10** and **11**, respectively. TSP (Trimethylsilyl-3-propionic acid sodium salt-D4, 99% D, Armar Scientific, Switzerland) was included into samples as internal standard for chemical shifts referencing (0.0 ppm). A canonical strategy was used to obtain proton resonance assignments [40]. Spectra were processed with VNMRJ 1.1D (Varian, Italy) and analyzed with the software NEASY [56] included in CARA (http://www.nmr.ch/).

NMR structures of **3**, **4**, **10** and **11** compounds were calculated using CYANA 2.1 [41]. Distance constraints were obtained from 2D [$^1$H, $^1$H] ROESY 250 spectra, and angular constraints with the GRIDSEARCH module of CYANA. The non-standard amino acids S-acetaminomethyl-L-cysteine (C(Acm)), 3-(1-naphthyl)-alanine (Nal1), L-Ornitine (Orn), and Homo Arginine (hArg) were generated with the software CYLIB [57] and included into CYANA standard residue library. Side chains of peptide residues performing the cyclization were also modified in the CYANA library, then the distance between Asp$^1$ CG and Lys$^9$ NZ atoms of peptide **3**, and **4**, Glu$^1$ CD and Orn$^9$ NE of peptide **10**, Glu$^1$ CD and Lys$^9$ NZ of peptide **11** was imposed equal to 1.33 Å during structure calculations. Structure calculations started from 100 random conformers, next the 20 structures with the lowest CYANA target functions were implemented in the software UCSF Chimera (version 1.10.1) [42] to carry out unrestrained energy minimizations. Minimization cycles were achieved through 1000 steps of steepest descent and 1000 steps of conjugate gradients [43]. Structures were additionally inspected with the program MOLMOL [58]. The "ensemble cluster module" of

UCSF Chimera was also employed to subdivide NMR conformers in subfamilies of conformationally related structures. The clusterization procedure was achieved by superimposing NMR structures on all atoms of all residues, excluding N-terminal acetylation and C-terminal amidation. Further details about Chimera clusterization protocol are available in Ref. [43].

### 4.5. Computational methods

Peptide starting models were built by homology by using as a template the NMR structure and protonation state of the analogue **2** [28], and the molefacture VMD plugin [59]. Peptides were then parameterized through the ATB server [60] to generate their GROMOS 54a7 topology [61] for the subsequent MD simulation. Free cyclic compounds were then minimized and placed in a cubic box with a SPC water layer of 0.7 nm. The system was further minimized. Minimizations were followed by 100ps long NVT and NPT equilibrations for 100 ps, and 1000ns long NPT production runs at 300 K. The iteration time step was set to 2 fs with the Verlet integrator and LINCS [62] constraint. We used periodic boundary conditions. The configurations were clustered with respect to their backbone arrangement with the single linkage method and cutoff 0.08 nm. For each peptide the representative conformation of the most populated cluster was then employed as starting conformation for subsequent docking to JAK2. Peptides were docked to JAK2 (PDB: 3FUP [63], chain A) with AutoDock Vina [64]. The (22.5x19.5x22.5)Å docking box was centered on KIR as of the JAK2/KIR complex constructed by following the procedure of Ref. [28]. The docking was performed with exhaustiveness 500 and energy range 50. Larger exhaustiveness ad energy ranges led to the same result. Peptide:JAK2 complexes then underwent the same MD procedure as that employed for the free peptides, with 500ns long production NPT runs. Contact area was calculated as the difference in solvent exposed surface areas between the free protein minus that attributed to the protein in the peptide:JAK2 complexes. Configurations were sampled every 100 ps. Datapoints were smoothed with a Bezier curve. All MD simulations and their analysis were run as implemented in the Gromacs package v. 2019.6 [65]. Simulations were run on high performance computing (HPC) resources hosted at the University of Trieste, University of Udine and CINECA Italy. Access to HPC infrastructures was carried out through the link https://www.hpc.cineca.it.

### 4.6. Serum stability of peptides

25% fetal bovine serum (FBS) was incubated at 37 °C for 15 min, with cyclic compounds (1 mg/mL, 700 μM at average) were added to the serum as previously described [24]. 50 μL aliquots of the incubating mixtures were recovered at different time intervals (0, 3, 17, 20, 23 and 42 h). Samples were treated with 50 μL of 30% trichloroacetic acid (TCA) and incubated at −20 °C for at least 20 min to precipitate serum proteins. The samples were subsequently centrifuged to remove serum proteins. RP-HPLC was performed on HPLC LC-4000 series (Jasco) with UV detector using a C18-Kinetek column from Phenomenex (Milan, Italy). Gradient elution was performed at 25 °C (monitoring at 210 nm) in a gradient starting with buffer A (0.1% TFA in $H_2O$) and applying buffer B (0.1% TFA in $CH_3CN$) from 5 to 70% in 20 min. The peak areas of recovered compounds over time were then integrated by assuming 100% their peak areas at t = 0 min.

## Author contributions

S.L.M., F.M., R.B. and I.D.D. synthesized and characterized the peptides. S.L.M. and I.D.D. performed CD and MST experiments. S.L.M. performed serum stability assay. M.L. and F.A.M. performed NMR experiments and solution structure calculations. S.F. performed computational analysis. D.M. and P.G. supervised the experiments. D.M. designed the concept and wrote the manuscript. All authors have given approval to the final version of the manuscript.


## Funding sources

This work was supported by Fondazione Italiana Sclerosi Multipla (FISM), project 2020/PR-Single/015 to D.M.


## Declaration of competing interest

The authors declare that they have no known competing financial interests or personal relationships that could have appeared to influence the work reported in this paper.

## Data availability

Data will be made available on request.


## Acknowledgment

Sara La Manna was supported by the AIRC fellowship for Italy. Rosa Bellavita was supported by Fondazione Umberto Veronesi. We acknowledge the CINECA Awards N. HP10CKYM0P, 2019, for the availability of high-performance computing re-sources and support.


## Appendix A. Supplementary data

Supplementary data to this article can be found online at https://doi.org/10.1016/j.ejmech.2022.114781.

## Abbreviations

| | |
|---|---|
| CD | Circular Dichroism |
| COPD | chronic obstructive pulmonary disease |
| Cys(Acm) | Acetaminomethyl-L-cysteine; |
| DQFCOSY | Double Quantum-Filtered Correlated Spectroscopy |
| EGTA | Egtazic acid |
| ESS | Extended SH2 Subdomain |
| FBS | Fetal Bovine Serum |
| IFN-γ, | Interferon gamma |
| IL, | Interleukin |
| JAK | Janus Kinases |
| KIR | Kinase Inhibitory Region |
| LC-MS | Liquid Chromatography Mass Spectrometry |
| LIF | leukemia inhibitory factor |
| MD | molecular dynamics |
| MST | Microscale Thermophoresis |
| Nal | Naphtylalanine; |
| NMR | Nuclear Magnetic Resonance |
| NOESY | Nuclear Overhauser Enhancement Spectroscopy |
| OSCC | oral squamous cell carcinoma |
| ROESY | Rotating Frame Overhauser Enhancement Spectroscopy |
| SAR | Structure-Activity Relationship; |
| SH2 | Src Homology 2 |
| SOCS | Suppressors Of Cytokine Signaling |
| SOD1 | superoxide dismutase 1 |
| STAT | Signal Transducer and Activator of Transcription |
| TCA | Trichloroacetic acid |
| TOCSY | Total Correlation Spectroscopy |
| TSP | Trimethylsilyl-3-propionic acid sodium salt-D4 |

## References


[1] K. Ghoreschi, A. Laurence, J.J. O'Shea, Janus kinases in immune cell signaling, Immunol. Rev. 228 (1) (2009) 273–287.

[2] H. Koldsø, M.S. Sansom, Signal transduction by a cytokine receptor: multi-scale computational studies of the membrane associated Gp130 receptor complex, Biophys. J. 104 (2) (2013) 608a.

[3] C. Banfield, M. Scaramozza, W. Zhang, E. Kieras, K.M. Page, A. Fensome, M. Vincent, M.E. Dowty, K. Goteti, P.J. Winkle, The safety, tolerability, pharmacokinetics, and pharmacodynamics of a TYK2/JAK1 inhibitor (PF-06700841) in healthy subjects and patients with plaque psoriasis, J. Clin. Pharmacol. 58 (4) (2018) 434–447.
[4] M. Fujimoto, H. Tsutsui, S. Yumikura-Futatsugi, H. Ueda, O. Xingshou, T. Abe, I. Kawase, K. Nakanishi, T. Kishimoto, T. Naka, A regulatory role for suppressor of cytokine signaling-1 in Th polarization in vivo, Int. Immunol. 14 (11) (2002) 1343–1350.
[5] J. Sharma, J. Larkin 3rd, Therapeutic implication of SOCS1 modulation in the treatment of autoimmunity and cancer, Front. Pharmacol. 10 (2019) 324.
[6] M. Federici, M.L. Giustizieri, C. Scarponi, G. Girolomoni, C. Albanesi, Impaired IFN-γ-dependent inflammatory responses in human keratinocytes overexpressing the suppressor of cytokine signaling 1, J. Immunol. 169 (1) (2002) 434–442.
[7] A. Sutra Del Galy, S. Menegatti, J. Fuentealba, F. Lucibello, L. Perrin, J. Helft, A. Darbois, M. Saitakis, J. Tosello, D. Rookhuizen, In vivo genome-wide CRISPR screens identify SOCS1 as intrinsic checkpoint of CD4+ TH1 cell response, Science Immunology 6 (66) (2021), eabe8219.
[8] R. Yao, Y.-L. Ma, W. Liang, H.-H. Li, Z.-J. Ma, X. Yu, Y.-H. Liao, MicroRNA-155 Modulates Treg and Th17 Cells Differentiation and Th17 Cell Function by Targeting SOCS.1, 2012.
[9] B. Sukka-Ganesh, Y. Li, W.H. Reeves, J. Larkin, Reduced Suppressor of Cytokine Signaling-1 levels in SLE patients correlates to enhanced STAT1 activation, Am Assoc Immnol (2016).
[10] S. La Manna, I. De Benedictis, D. Marasco, Proteomimetics of natural regulators of JAK-STAT pathway: novel therapeutic perspectives, Front. Mol. Biosci. 8 (2021), 792546.
[11] K. Nakatani, S. Serada, M. Fujimoto, K. Obata, T. Ohkawara, E. Sasabe, T. Yamamoto, T. Naka, Gene therapy with SOCS1 induces potent preclinical antitumor activities in oral squamous cell carcinoma, J. Oral Pathol. Med. 51 (2) (2022) 126–133.
[12] E.M. Linossi, S.E. Nicholson, The SOCS box-adapting proteins for ubiquitination and proteasomal degradation, IUBMB Life 64 (4) (2012) 316–323.
[13] E.M. Linossi, J.J. Babon, D.J. Hilton, S.E. Nicholson, Suppression of cytokine signaling: the SOCS perspective, Cytokine Growth Factor Rev. 24 (3) (2013) 241–248.
[14] M.M. Song, K. Shuai, The suppressor of cytokine signaling (SOCS) 1 and SOCS3 but not SOCS2 proteins inhibit interferon-mediated antiviral and antiproliferative activities, J. Biol. Chem. 273 (52) (1998) 35056–35062.
[15] N.P.D. Liau, A. Laktyushin, I.S. Lucet, J.M. Murphy, S. Yao, E. Whitlock, K. Callaghan, N.A. Nicola, N.J. Kershaw, J.J. Babon, The molecular basis of JAK/STAT inhibition by SOCS1, Nat. Commun. 9 (1) (2018) 1558.
[16] Y. Wei, Z. Zhang, N. She, X. Chen, Y. Zhao, J. Zhang, Atomistic insight into the inhibition mechanisms of suppressors of cytokine signaling on Janus kinase, Phys. Chem. Chem. Phys. 21 (24) (2019) 12905–12915.
[17] D. Marasco, G. Perretta, M. Sabatella, M. Ruvo, Past and future perspectives of synthetic peptide libraries, Curr. Protein Pept. Sci. 9 (5) (2008) 447–467.
[18] E. Lonardo, C.L. Parish, S. Ponticelli, D. Marasco, D. Ribeiro, M. Ruvo, S. De Falco, E. Arenas, G. Minchiotti, A small synthetic cripto blocking Peptide improves neural induction, dopaminergic differentiation, and functional integration of mouse embryonic stem cells in a rat model of Parkinson's disease, Stem Cell. 28 (8) (2010) 1326–1337.
[19] S. Ponticelli, D. Marasco, V. Tarallo, R.J. Albuquerque, S. Mitola, A. Takeda, J. M. Stassen, M. Presta, J. Ambati, M. Ruvo, S. De Falco, Modulation of angiogenesis by a tetrameric tripeptide that antagonizes vascular endothelial growth factor receptor 1, J. Biol. Chem. 283 (49) (2008) 34250–34259.
[20] S. Madonna, C. Scarponi, N. Doti, T. Carbone, A. Cavani, P.L. Scognamiglio, D. Marasco, C. Albanesi, Therapeutical potential of a peptide mimicking the SOCS1 kinase inhibitory region in skin immune responses, Eur. J. Immunol. 43 (7) (2013) 1883–1895.
[21] N. Doti, P.L. Scognamiglio, S. Madonna, C. Scarponi, M. Ruvo, G. Perretta, C. Albanesi, D. Marasco, New mimetic peptides of the kinase-inhibitory region (KIR) of SOCS1 through focused peptide libraries, Biochem. J. 443 (1) (2012) 231–240.
[22] S. La Manna, P.L. Scognamiglio, C. Di Natale, M. Leone, F.A. Mercurio, A. M. Malfitano, F. Cianfarani, S. Madonna, S. Caravella, C. Albanesi, E. Novellino, D. Marasco, Characterization of linear mimetic peptides of Interleukin-22 from dissection of protein interfaces, Biochimie 138 (2017) 106–115.
[23] S. La Manna, L. Lopez-Sanz, S. Bernal, L. Jimenez-Castilla, I. Prieto, G. Morelli, C. Gomez-Guerrero, D. Marasco, Antioxidant effects of PS5, a peptidomimetic of suppressor of cytokine signaling 1, Experimental Atherosclerosis, Antioxidants (Basel) 9 (8) (2020).
[24] S. La Manna, L. Lopez-Sanz, M. Leone, P. Brandi, P.L. Scognamiglio, G. Morelli, E. Novellino, C. Gomez-Guerrero, D. Marasco, Structure-activity studies of peptidomimetics based on kinase-inhibitory region of suppressors of cytokine signaling 1, Biopolymers (2017).
[25] P.L. Scognamiglio, C. Di Natale, G. Perretta, D. Marasco, From peptides to small molecules: an intriguing but intricated way to new drugs, Curr. Med. Chem. 20 (31) (2013) 3803–3817.
[26] S. La Manna, C. Di Natale, D. Florio, D. Marasco, Peptides as therapeutic agents for inflammatory-related diseases, Int. J. Mol. Sci. 19 (9) (2018).
[27] A. Russo, C. Aiello, P. Grieco, D. Marasco, Targeting "undruggable" proteins: design of synthetic cyclopeptides, Curr. Med. Chem. 23 (8) (2016) 748–762.
[28] S. La Manna, L. Lopez-Sanz, S. Bernal, S. Fortuna, F.A. Mercurio, M. Leone, C. Gomez-Guerrero, D. Marasco, Cyclic mimetics of kinase-inhibitory region of Suppressors of Cytokine Signaling 1: progress toward novel anti-inflammatory therapeutics, Eur. J. Med. Chem. 221 (2021), 113547.
[29] S. Fung, V.J. Hruby, Design of cyclic and other templates for potent and selective peptide alpha-MSH analogues, Curr. Opin. Chem. Biol. 9 (4) (2005) 352–358.
[30] O. Van der Poorten, A. Knuhtsen, D. Sejer Pedersen, S. Ballet, D. Tourwe, Side chain cyclized aromatic amino acids: great tools as local constraints in peptide and peptidomimetic design, J. Med. Chem. 59 (24) (2016) 10865–10890.
[31] F. Merlino, Y. Zhou, M. Cai, A. Carotenuto, A.M. Yousif, D. Brancaccio, S. Di Maro, S. Zappavigna, A. Limatola, E. Novellino, P. Grieco, V.J. Hruby, Development of macrocyclic peptidomimetics containing constrained alpha,alpha-dialkylated amino acids with potent and selective activity at human melanocortin receptors, J. Med. Chem. 61 (9) (2018) 4263–4269.
[32] D.F. Mierke, G. Nossner, P.W. Schiller, M. Goodman, Morphiceptin analogs containing 2-aminocyclopentane carboxylic acid as a peptidomimetic for proline, Int. J. Pept. Protein Res. 35 (1) (1990) 35–45.
[33] G. Ballano, D. Zanuy, A.I. Jiménez, C. Cativiela, R. Nussinov, C. Alemán, Structural analysis of a β-helical protein motif stabilized by targeted replacements with conformationally constrained amino acids, J. Phys. Chem. B 112 (41) (2008) 13101–13115.
[34] C.T. Walsh, R.V. O'Brien, C. Khosla, Nonproteinogenic amino acid building blocks for nonribosomal peptide and hybrid polyketide scaffolds, Angew Chem. Int. Ed. Engl. 52 (28) (2013) 7098–7124.
[35] M. Jerabek-Willemsen, C.J. Wienken, D. Braun, P. Baaske, S. Duhr, Molecular interaction studies using microscale thermophoresis, Assay Drug Dev. Technol. 9 (4) (2011) 342–353.
[36] P. Fortuna, A. Twarda-Clapa, L. Skalniak, K. Ożga, T.A. Holak, Ł. Berlicki, Systematic 'foldamerization' of peptide inhibiting p53-MDM2/X interactions by the incorporation of trans-or cis-2-aminocyclopentanecarboxylic acid residues, Eur. J. Med. Chem. 208 (2020), 112814.
[37] C. Griesinger, G. Otting, K. Wuthrich, R.R. Ernst, Clean tocsy for H-1 spin system-identification in macromolecules, J. Am. Chem. Soc. 110 (23) (1988) 7870–7872.
[38] A. Bax, D.G. Davis, Practical aspects of two-dimensional transverse noe spectroscopy, J. Magn. Reson. 63 (1) (1985) 207–213.
[39] A. Kumar, R.R. Ernst, K. Wuthrich, A two-dimensional nuclear Overhauser enhancement (2D NOE) experiment for the elucidation of complete proton-proton cross-relaxation networks in biological macromolecules, Biochem. Biophys. Res. Commun. 95 (1) (1980) 1–6.
[40] K. Wuthrich, NMR of Proteins and Nucleic Acids, Wiley, New York, 1986.
[41] T. Herrmann, P. Guntert, K. Wuthrich, Protein NMR structure determination with automated NOE assignment using the new software CANDID and the torsion angle dynamics algorithm DYANA, J. Mol. Biol. 319 (1) (2002) 209–227.
[42] E.F. Pettersen, T.D. Goddard, C.C. Huang, G.S. Couch, D.M. Greenblatt, E.C. Meng, T.E. Ferrin, UCSF Chimera–a visualization system for exploratory research and analysis, J. Comput. Chem. 25 (13) (2004) 1605–1612.
[43] L.A. Kelley, S.P. Gardner, M.J. Sutcliffe, An automated approach for clustering an ensemble of NMR-derived protein structures into conformationally related subfamilies, Protein Eng. 9 (11) (1996) 1063–1065.
[44] S.-x. Liao, J. Chen, L.-Y. Zhang, J. Zhang, P.-P. Sun, Y. Ou-Yang, Effects of SOCS1-overexpressing dendritic cells on Th17-and Treg-related cytokines in COPD mice, BMC Pulm. Med. 22 (1) (2022) 1–18.
[45] J.-Y. Ryu, J. Oh, S.-M. Kim, W.-G. Kim, H. Jeong, S.-A. Ahn, S.-H. Kim, J.-Y. Jang, B.C. Yoo, C.W. Kim, SOCS1 Counteracts ROS-Mediated Survival Signals and Promotes Apoptosis by Modulating Cell Cycle to Increase Radiosensitivity of Colorectal Cancer Cells, BMB reports, 2022.
[46] C.M. Ahmed, J. Larkin 3rd, H.M. Johnson, SOCS1 mimetics and antagonists: a complementary approach to positive and negative regulation of immune function, Front. Immunol. 6 (2015) 183.
[47] J. Sharma, T.D. Collins, T. Roach, S. Mishra, B.K. Lam, Z.S. Mohamed, A.E. Veal, T. B. Polk, A. Jones, C. Cornaby, M.I. Haider, L. Zeumer-Spataro, H.M. Johnson, L. M. Morel, J. Larkin 3rd, Suppressor of cytokine signaling-1 mimetic peptides attenuate lymphocyte activation in the MRL/lpr mouse autoimmune model, Sci. Rep. 11 (1) (2021) 6354.
[48] C.E. Plummer, T. Polk, J. Sharma, S.S. Bae, O. Barr, A. Jones, H. Kitchen, M. Wilhelmy, K. Devin, W. Clay Smith, Open label safety and efficacy pilot to study mitigation of equine recurrent uveitis through topical suppressor of cytokine signaling-1 mimetic peptide, Sci. Rep. 12 (1) (2022) 1–11.
[49] H. Chen, Y. Wu, K. Li, I. Currie, N. Keating, F. Dehkhoda, C. Grohmann, J.J. Babon, S.E. Nicholson, B.E. Sleebs, Optimization of phosphotyrosine peptides that target the SH2 domain of SOCS1 and block substrate ubiquitination, ACS Chem. Biol. (2022).
[50] F. Merlino, S. Tomassi, A.M. Yousif, A. Messere, L. Marinelli, P. Grieco, E. Novellino, S. Cosconati, S. Di Maro, Boosting Fmoc solid-phase peptide synthesis by ultrasonication, Org. Lett. 21 (16) (2019) 6378–6382.
[51] S. La Manna, L. Lopez-Sanz, F.A. Mercurio, S. Fortuna, M. Leone, C. Gomez-Guerrero, D. Marasco, Chimeric peptidomimetics of SOCS 3 able to interact with JAK2 as anti-inflammatory compounds, ACS Med. Chem. Lett. 11 (5) (2020) 615–623.
[52] L. Hellinen, S. Bahrpeyma, A.K. Rimpela, M. Hagstrom, M. Reinisalo, A. Urtti, Microscale thermophoresis as a screening tool to predict melanin binding of drugs, Pharmaceutics 12 (6) (2020).
[53] A. Micsonai, F. Wien, L. Kernya, Y.H. Lee, Y. Goto, M. Refregiers, J. Kardos, Accurate secondary structure prediction and fold recognition for circular dichroism spectroscopy, Proc. Natl. Acad. Sci. U.S.A. 112 (24) (2015) E3095–E3103.
[54] U. Piantini, O.W. Sorensen, R.R. Ernst, Multiple quantum filters for elucidating NMR coupling networks, J. Am. Chem. Soc. 104 (24) (1982) 6800–6801.

[55] T.L. Hwang, A.J. Shaka, Water suppression that works - excitation sculpting using arbitrary wave-forms and pulsed-field gradients, J. Magn. Reson., Ser. A 112 (2) (1995) 275–279.
[56] C. Bartels, T.H. Xia, M. Billeter, P. Guntert, K. Wuthrich, The program XEASY for computer-supported NMR spectral analysis of biological macromolecules, J. Biomol. NMR 6 (1) (1995) 1–10.
[57] E.M. Yilmaz, P. Guntert, NMR structure calculation for all small molecule ligands and non-standard residues from the PDB Chemical Component Dictionary, J. Biomol. NMR 63 (1) (2015) 21–37.
[58] R. Koradi, M. Billeter, K. Wuthrich, MOLMOL: a program for display and analysis of macromolecular structures, J. Mol. Graph. 14 (1) (1996) 29–32, 51-5.
[59] W. Humphrey, A. Dalke, K. Schulten, VMD: visual molecular dynamics, J. Mol. Graph. 14 (1) (1996) 33–38.
[60] A.K. Malde, L. Zuo, M. Breeze, M. Stroet, D. Poger, P.C. Nair, C. Oostenbrink, A. E. Mark, An automated force field topology builder (ATB) and repository: version 1.0, J. Chem. Theor. Comput. 7 (12) (2011) 4026–4037.
[61] C. Oostenbrink, A. Villa, A.E. Mark, W.F. Van Gunsteren, A biomolecular force field based on the free enthalpy of hydration and solvation: the GROMOS force-field parameter sets 53A5 and 53A6, J. Comput. Chem. 25 (13) (2004) 1656–1676.
[62] B. Hess, H. Bekker, H.J. Berendsen, J.G. Fraaije, LINCS: a linear constraint solver for molecular simulations, J. Comput. Chem. 18 (12) (1997) 1463–1472.
[63] N.K. Williams, R.S. Bamert, O. Patel, C. Wang, P.M. Walden, A.F. Wilks, E. Fantino, J. Rossjohn, I.S. Lucet, Dissecting specificity in the Janus kinases: the structures of JAK-specific inhibitors complexed to the JAK1 and JAK2 protein tyrosine kinase domains, J. Mol. Biol. 387 (1) (2009) 219–232.
[64] O. Trott, A.J. Olson, AutoDock Vina, Improving the speed and accuracy of docking with a new scoring function, efficient optimization, and multithreading, J. Comput. Chem. 31 (2) (2010) 455–461.
[65] S. Pronk, S. Páll, R. Schulz, P. Larsson, P. Bjelkmar, R. Apostolov, M.R. Shirts, J. C. Smith, P.M. Kasson, D. van der Spoel, Gromacs 4.5: a high-throughput and highly parallel open source molecular simulation toolkit, Bioinformatics 29 (7) (2013) 845–854.